

Preparation and Photocatalytic Activity of Coatings based on Size-selective V-TiO₂ Nanoparticles

Miguel Sanchez Mendez^a, Alex Lemarchand^a, Mamadou Traore^a, Mounir Ben Amar^a, Christian Perruchot^b, Mehrdad Nikravech^a, Andrei Kanaev^a

^aLaboratoire des Sciences des Procédés et des Matériaux, CNRS, Université Sorbonne Paris Nord, 93430 Villetaneuse, France

^bLaboratoire Interfaces Traitements Organisation et Dynamique des Systèmes, CNRS, Université de Paris, F-75013 Paris, France

andrei.kanaev@lspm.cnrs.fr

Titanium-vanadium oxo-alkoxy (VTOA) nanoparticles with vanadium addition (V:Ti) between 0 and 20 mol% were prepared via sol-gel method in a chemical reactor with ultra-rapid micromixing. A control of the nucleation and growth process in the reactor permitted synthesis of size-selective V-TiO₂ nanoparticles, which were used for the nanocoatings deposition on glass beads. The activity of the prepared photocatalysts (after calcination at 450 °C) was studied by the degradation of methylene blue in aqueous solutions under UVA illumination. A steady decrease of the reaction rate was observed with an increase of the vanadium content. This effect was explained by the residual presence of non-crystallized oxide, which elimination requires further studies.

1. Introduction

Photocatalysis has deserved a growing interest as an important solution to clean water, air and soils from toxic contaminants over the last decades (Ohtani, 2010; Parrino et al., 2018). One of key materials in this connection became titanium dioxide (TiO₂) (Hashimoto et al., 2005), which has shown high effectiveness in the environmental process. Its main shortcoming, however, consists in a relatively rapid charge recombination reducing the energetic efficiency and activation under UVA light illumination (Banerjee et al. 2014). Much effort has been done in the solution of the above problem by doping titanium dioxide with metal cation (Ag, Fe, V, Au, Pt, etc.) and non-metallic element (N, S, C, B, P, etc.) (Zaleska A., 2008; Schneider et al., 2014).

Vanadium pentoxide (V₂O₅) is a potentially interesting material for photocatalytic applications because of its significantly narrower band-gap of 2.2 eV (compared to 3.2 eV of anatase TiO₂), which allows the process activation with visible light of wavelengths as long as 560 nm (Kruefu et al., 2017). In the same time, this pure material suffered from a high probability of the photogenerated electron-hole pair recombination, which limits perspectives of the implementation. On a way to overcome the limitations, different compositions of V₂O₅ with other semiconductors have been investigated: V₂O₅/SiO₂ (Amano et al., 2004), V₂O₅/BiVO₄ (Su et al., 2011), V₂O₅/Al₂O₃ (Teramura et al., 2009) and TiO₂/V₂O₅ (Jianhua et al., 2006).

Bettinelli et al. (2007) have synthesized V-doped TiO₂ photocatalysts via a modified sol-gel process reporting that the activity was significantly affected by preparation conditions. They have explained that the surface vanadium caused the pollutant (methylene blue, MB) degradation, while the bulk vanadium did not influence the activity; in the same time, surface vanadium also caused the deactivation, suggesting the presence of poisoning effects. Chang et al. (2009) have reported a red-shift of the absorption onset energy of V-TiO₂ nanoparticles with V content up to ~2 wt% prepared via sol-gel method. They have observed a moderate decrease of the MB decomposition rate under UV light illumination (305 nm); in the same time, a significant increase of the decomposition rate was observed under the solar simulator illumination with the optimum attained at the V content of 0.5-1 wt%. Lin and Lin (2012) have shown that an optimal vanadium content of 5% enhanced the pseudo first order photocatalytic kinetics of MB degradation under the visible light irradiation, which was explained by the migration of photogenerated electrons to vanadium, thus improving the electron-

hole separation; moreover, V-doping of TiO₂ increased the crystal grain size affecting specific surface areas of powders and extended the material absorption in the spectral range of 400-800 nm. Khan and Berk (2013) have reported a successful incorporation of V⁵⁺ ions into the TiO₂ crystalline lattice that resulted in a decrease of the band-gap energy and a decrease in photogenerated electrons and holes recombination rate. These and other recent studies on V-TiO₂ have indicated an optimal material composition for the best photocatalytic performance (Al-Mamun et al., 2019). While optimisation of the photocatalyst composition and morphology advances, the relevant problem concerns development of the photocatalysis preparation process (Meramo et al., 2018; Stoller et al., 2019). A chemical reactor with ultrarapid micromixing of the reactive fluids has been previously developed in our group for the mass-fabrication of size-selected pure, doped and mixed metal oxide nanoparticles, and its performance has been demonstrated on the preparation of TiO₂, Zr_xTi_{1-x}O₂ photocatalytic nanoparticles and nanocoatings (Azouani et al., 2009; Azouani et al., 2010; Cheng et al., 2017; Cheng et al., 2018). In this work, we extend studies to the photocatalytic activity of V-TiO₂ nanoparticles prepared via sol-gel method in the dedicated chemical reactor.

2. Experimental

2.1 Photocatalyst preparation

The mixed oxide V-TiO₂ nanoparticles with different vanadium addition (V:Ti) between 0 and 20 mol% were prepared in a laboratory chemical reactor with ultrarapid micromixing of the reacted precursors (Rivallin et al., 2005, Azouani et al., 2010), followed by the reactive colloid deposition on glass beads and heat treatment. The vanadium-titanium-oxo-alkoxy (VTOA) nanoparticles were generated using sol-gel method, as this has been previously reported (Sanchez Mendez et al., 2019). The two stock solutions (each of 50 ml volume) injected into the reactor contained respectively A) mixed vanadium oxytriisopropoxide (98%, Sigma Aldrich) and titanium tetraisopropoxide (TTIP, 98%, Sigma-Aldrich) precursors in n-propanol (99.5%, Sigma Aldrich) and B) twice filtered distilled water (syringe filter 0.1 μm porosity PALLs Acrodisc) in n-propanol. The titanium precursor concentration in the reaction volume was C_{Ti}=0.3 mol/l and water concentration C_w was adjusted in order to maintain the hydrolysis ratio $H=C_w/(C_{Ti}+C_v)=1.5$, which assures the nucleation but prohibits the particles growth. The reactor was maintained at the temperature of 20 °C with a thermo-cryostat Haake DC10K15. The reactor operated at the Damköhler number $Da \leq 1$, which means that the reaction medium was perfectly homogeneous before the chemical reactions leading to nucleation of species occurred, which permits the narrowest polydispersity of the produced nanoparticles. The nanoparticles generated in the reactor were deposited on glass beads of 4 mm diameter (Supelco, Merck) via liquid colloid deposition method under controlled atmosphere in a LABstar glove box workstation MBraun (O₂ ≤ 80 ppm, H₂O ≤ 0.5 ppm). Before deposition, the beads were washed in sulfuric acid for 1 day, rinsed in water until pH reached 7.0 and dried in oven at 80 °C for 12 h. After the deposition, the beads are separated from the solution, dried overnight in the glove box and heat treated at 450 °C for 4 hours.

The TGA-DTA measurements of the prepared nanoparticles were carried out with Labsys Evo de SETARAM at the air flow and heating rate of 10 °C/min. The samples were structurally characterized by X-ray diffraction (XRD) method on INEL XRG 3000 installation using Co-Kα₁ (λ=1.789 Å) radiation source. The photocatalytic tests were conducted in the reactor with a closed circulating loop depicted in Figure 1.

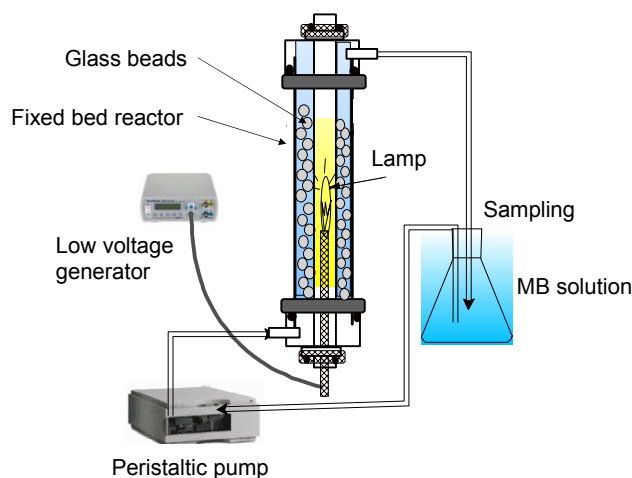


Figure 1: Schema of the photocatalytic reactor.

The coated glass beads ($m=90$ g, $N=1050$ pieces) were freely placed in a gap of 6 mm width between two cylinder quartz tubes of lengths 395 mm. The inner tube of 34 mm external diameter contained 8-W power UVA lamp, emitting at 365 nm with full-width at half maximum $\Delta\lambda_{1/2}=15$ nm, of 16 mm diameter and 395 mm length, equal to that of the surrounding quartz tubes. As a model pollutant, we used methylene blue (MB) solution in water at concentration $C_{MB}=1.0 \cdot 10^{-5}$ mol. The circulated liquid with the total volume of 400 ml was stocked in a reservoir and pushed with a flow rate of 300 ml/min by a peristaltic pump unit. The UV-visible absorption spectra of MB in the solution were taken at the outlet of the reactor bed (before entering the reservoir) by using an optical fiber-coupled compact AvaSpec UV-visible spectrometer with spectral resolution of 0.5 nm. The experiments were conducted in two steps. On the first step, adsorption spectra of MB were measured in a dark during 3 hours until reaching the adsorption-desorption equilibrium at the photocatalyst surface. On the second step, the UV-lamp was turned on and MB spectra were measured during the pollutant decomposition during 3 hours. Besides of V-TiO₂ nanocoatings, blank tests were carried out on the empty reactor and on the reactor filled with uncoated glass beads in order to evaluate contributions of the direct photolysis of free and adsorbed MB by UVA-lamp photons. The MB concentration was obtained from the absorption spectra maximum at 666 nm. The reproducibility of the experimental series was verified.

3. Results and Discussion

As we have recently shown (Sanchez Mendez et al., 2020), at a relatively low V content ≤ 0.20 mol% the VTOA nanoparticles are formed via the condensation of titanium oxo-alkoxy (TOA) species, which attract hydrolysed vanadium species at the surface. In contrast, at the higher V content hydrolyzed vanadium oxo-alkoxy (VOA) species imprison subnucleus condensed TOA species prohibiting the nucleation. Therefore, the vanadium content in the present study was limited to 20 mol%.

The results of TGA-DTA measurements of the selected nanopowders produced in the chemical reactor (non-treated thermally) are shown in Figure 2. In all presented patterns, the broad endothermic peak between 50 °C and ~200 °C with the maximum at 150 °C was observed, which is due to desorption of solvent release from the particles surface, followed by another broad exothermic band with the maximum at ~250 °C due to the residual organics burning. We can notice a much stronger fraction of the desorbed mass in mixed oxide nanoparticles compared with that in pure titania, which may be due to a stronger retention of the adsorbed solvent by the mixed oxides species. However the most significant modification concerns the strong exothermic peak due to the anatase phase crystallization appeared in pure titania at 414 °C (a). The peak significantly weakened and broadened in V-TiO₂ with 5 mol% vanadium (b) and intensified and narrowed with the further increase of the V content (c).

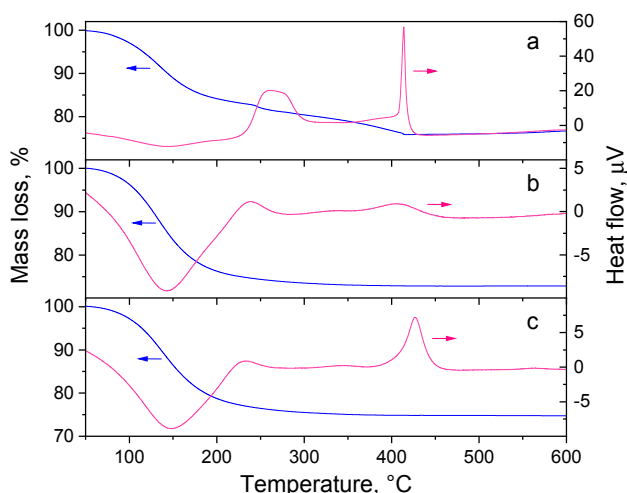


Figure 2: TGA (left) and DTA (right) measurements of TiO₂ (a) and V-TiO₂ samples with 5 mol% (b) and 10 mol% (c) vanadium.

The XRD patterns of selected nanopowders are shown in Figure 3. Although pure anatase phase was observed in all prepared samples, the peaks of V-TiO₂ were broadened compared to those of pure TiO₂, which corresponded to a small decrease of the crystallite size from ~11 nm (0 mol% V) to 7.5 nm (5 mol% V) and 9.5 nm (10 mol% V). According to our recent results (Sanchez Mendez et al., 2020), addition of vanadium

increases the size of VTAO nucleus. The XRD crystallite size decrease together with the strong DTA peaks broadening could be connected to the incomplete crystallization of the V-TiO₂ samples.

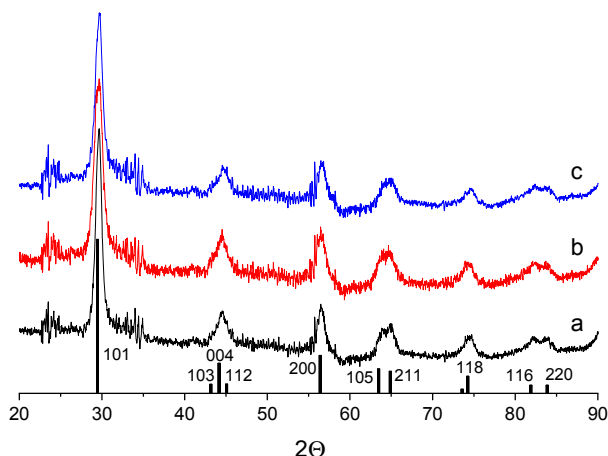


Figure 3: XRD powder patterns of TiO₂ (a) and V-TiO₂ samples with 5 mol% (b) and 10 mol% (c) vanadium. Vertical bars show positions and heights of anatase TiO₂ peaks.

The adsorption measurements of the selected samples are shown in Figure 4. Two groups of the curves can be distinguished. In fact, when there are no MB losses in non-illuminated empty reactor, ~50 mol% of MB was adsorbed on the uncoated glass beads at equilibrium. In contrast, about 25 mol% MB was adsorbed by the coated beads regardless of composition of the coated V-TiO₂ material.

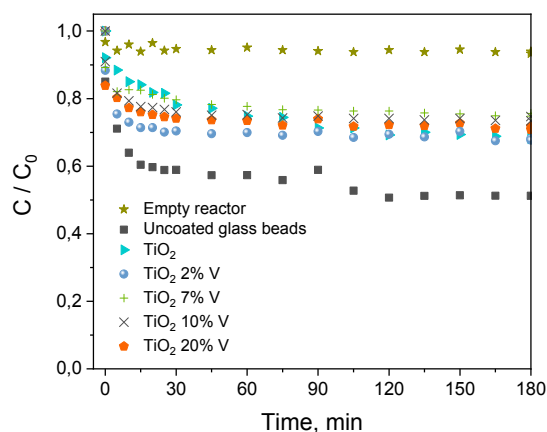


Figure 4: MB adsorption on V-TiO₂ coated glass beads, uncoated glass beads and in empty reactor.

The adsorption measurements permit distinguishing free and adsorbed MB exposed to UVA illumination in the photocatalytic tests and, consequently, their respective contributions to the MB photolysis. The kinetics of MB decomposition under UVA illumination in the empty reactor and that filled with uncoated clean and coated glass beads with TiO₂ nanoparticles is presented in Figure 5. One can see from these data that the photolysis of solvated MB molecules (empty reactor) is almost negligible in our experimental conditions. In contrast, adsorbed MB molecules (uncoated glass beads) underwent an appreciable photolytic decomposition. Consequently, we assumed that MB decomposition kinetics due to photolysis is directly proportional to the adsorbed MB quantity at equilibrium obtained from Figure 4. As a result, the photolytic rate in presence of the prepared photocatalysts was about a half of that in presence of uncoated glass beads. We also notice that a significant deactivation of TiO₂ photocatalyst takes place by the MB decomposition (second use). Studies of the deactivation process and methods of the catalyst recovery are under way.

The MB decomposition kinetics using V-TiO₂ nanocoatings with different elemental compositions are shown in Figure 6. The results clearly evidence the activity decrease with an increase of V content. Our particular method of the controlled V-TiO₂ nucleation (Sanchez Mendez et al., 2020), suggests the formation of particles enriched with surface vanadium, which should promote the photocatalytic activity (Bettinelli et al., 2007).

Unfortunately, our results do not allow neither confirming nor reject this assumption. In fact, according to Chang et al. (2009): (i) optimum V loading may be smaller than 2 mol% and (ii) losses of the activity under UVA illumination can be accompanied by the activity increase under visible light illumination. Moreover, unaccounted contamination of V-TiO₂ photocatalyst by the amorphous material due to the incomplete crystallisation can reduce the activity (Ohtani et al., 1997).

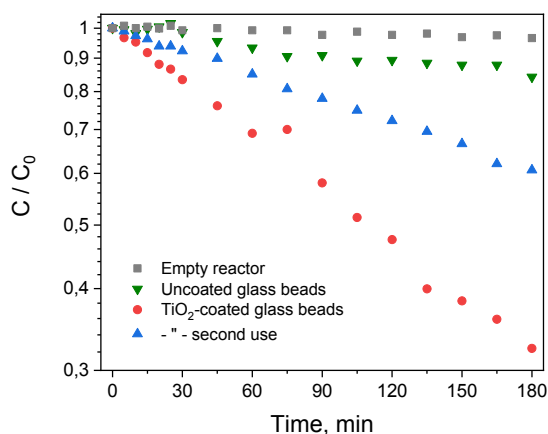


Figure 5: Kinetics of MB decomposition in the photocatalytic reactor: empty and filled with uncoated and coated glass beads with TiO₂ nanoparticles (1st and 2nd runs).

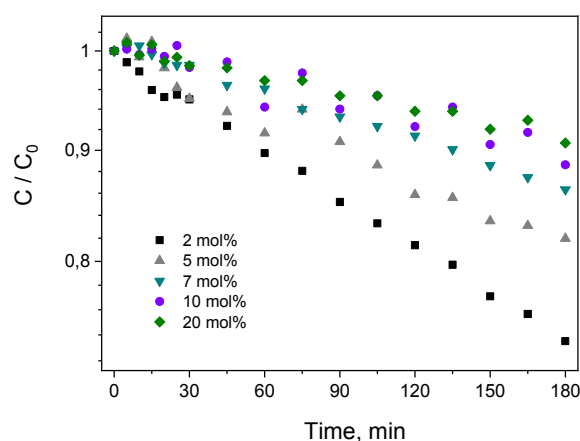


Figure 6: Kinetics of MB decomposition in photocatalytic reactor filled with V-TiO₂-coated glass beads.

4. Conclusions

Summing up, photocatalytic nano-coatings based on size-selected V-TiO₂ nanoparticles (0 ≤ V:Ti ≤ 0.2) were prepared via sol-gel method in a chemical reactor with ultra-rapid micromixing, followed by the chemical colloid deposition on borosilicate glass beads and thermal treatment at 450 °C for 4 hours. This method assured a homogeneous material composition at nanoscale ≤ 4 nm (defined by nucleus size). The activity of the prepared photocatalysts was studied by the degradation of methylene blue in aqueous solutions under UVA illumination. A decrease of the reaction rate was observed with an increase of the vanadium content, which was explained by a presence of residual non-crystallized material. The direct photolysis of the adsorbed MB molecules and photocatalytic decomposition of MB molecules were distinguished.

Acknowledgments

Miguel Sánchez Méndez acknowledges a financial support of his PhD work by the National Council of Science and Technology (CONACYT) of the Mexican government and the Doctoral School of the Sorbonne Paris-Nord University.

References

- Al-Mamun M.R., Kader S., Islam M.S., Khan M.Z.H., 2019, Photocatalytic activity improvement and application of UV-TiO₂ photocatalysis in textile wastewater treatment: A review, *J. Environ. Chem. Eng.*, 7, 103248.
- Amano F., Tanaka T., Funabiki T., 2004, Steady-state photocatalytic epoxidation of propene by O₂ over V₂O₅/SiO₂ photocatalysts, *Langmuir*, 20, 4236-4240.
- Azouani R., Tieng S., Michau A., Hassouni K., Chhor K., Bocquet J.-F., Vignes J.-L. and Kanaev A., 2009, Elaboration of Doped and composite nano-TiO₂, *Chem. Eng. Trans.*, 17, 981-986.
- Azouani R., Michau A., Hassouni K., Chhor K., Bocquet J.-F., Vignes J.-L. and Kanaev A., 2010, Elaboration of pure and doped TiO₂ nanoparticles in sol-gel reactor with turbulent micromixing: Application to nanocoatings and photocatalysis, *Chem. Eng. Res. Des.*, 88, 1123-1130.
- Banerjee S., Pillai S.C., Falaras P., O'Shea K.E., Byrne J.A., Dionysiou D.D., 2014, New insights into the mechanism of visible light photocatalysis, *Phys. Chem. Lett.*, 5, 2543-2554.
- Bettinelli M., Dallacasa V., Falcomer D., Fornasiero P., Gombac V., Montini T., Romano L., Speghini A., 2007, Photocatalytic activity of TiO₂ doped with boron and vanadium, *J. Hazard. Mater.*, 146, 529-534.
- Chang P-Y., Huang C-H, and Doong R-A, 2009, Characterization and photocatalytic activity of vanadium-doped titanium dioxide nanocatalysts, *Water Sci. Technol.*, 59, 523-530.
- Cheng K., Chhor K., and Kanaev A., 2018, Photocatalytic nanoparticulate Zr_xTi_{1-x}O₂ coatings with controlled homogeneity of elemental composition, *Chem. Select*, 3, 11118-11126.
- Cheng K., Chhor K., Brinza O., Vrel D., and Kanaev A., 2017, From nanoparticles to bulk crystalline solid: Nucleation, growth kinetics and crystallisation of mixed oxide Zr_xTi_{1-x}O₂ nanoparticles, *Cryst. Eng. Comm.*, 19, 3955-3965.
- Hashimoto K., Irie H., Fujishima A. 2005, TiO₂ photocatalysis: A historical overview and future prospects, *Jap. J. Appl. Phys.*, 44, 8269-8285.
- Jianhua L., Rong Y. and Songmei L., 2006, Preparation and characterization of the TiO₂/V₂O₅ photocatalyst with visible light activity, *Rare Metals.*, 25, 636-642.
- Khan H., Berk D., 2013, Sol-gel synthesized vanadium doped TiO₂ photocatalyst: physicochemical properties and visible light photocatalytic studies, *J. Sol-Gel Sci. Technol.*, 68, 180-192.
- Kruefu V., Sintuya H., Pookmanee P., Phanichphant S., 2017, Visible light photocatalytic degradation of methylene blue using V₂O₅ nanoparticles, *Proc. 6th Int. Conf. Dev. Eng. Technol.*, 62-67.
- Lin W-C., Lin Y-J., 2012, Effect of vanadium(IV)-doping on the visible light-induced catalytic activity of titanium dioxide catalysts for methylene blue degradation, *Environ. Eng. Sci.*, 29, 447-452
- Meramo S. I., Bonfante-Alvarez H., Avila-Montiel G. D., Herrera-Barros A, Gonzales-Delgado A. D., 2018, Environmental assessment of a large-scale production of TiO₂ nanoparticles via green chemistry, *Chem. Eng. Trans.*, 70, 1063-1068.
- Ohtani B., 2010, Photocatalysis A to Z - What we know and what we do not know in a scientific sense, *J. Photochem. Photobiol. C*, 11, 157-178.
- Ohtani B., Ogawa Y., Nishimoto S., 1997, Photocatalytic activity of amorphous-anatase mixture of titanium(IV) oxide particles suspended in aqueous solutions, *J. Phys. Chem. B*, 101, 3746-3752.
- Parrino F., Loddo V., Augugliaro V., Camera-Roda G., Palmisano G., Palmisano L., Yurdakal S., 2018, Heterogeneous photocatalysis: guidelines on experimental setup, catalyst characterization, interpretation, and assessment of reactivity, *Catal. Rev.*, 61, 163-213.
- Rivallin M., Benmami M., Kanaev A., Gaunand A., 2005, Sol-gel reactor with rapid micromixing: modelling and measurements of titanium oxide nano-particle growth, 83, 1, 67-74
- Sanchez Mendez M., Jia Z., Traore M., Ben Amar M., Nikravech M., Kanaev A., 2021, Nucleation and growth of mixed vanadium-titanium oxo-alkoxy nanoparticles in sol-gel synthesis, *Colloids. Surf. A*, 610, 125636
- Sanchez Mendez M., Cheng, K., Traore M., Ben Amar M., Kanaev A., 2019, Elaboration of mixed oxide photocatalysts, *Chem. Eng. Trans.*, 74, 433-438.
- Schneider J., Matsuoka M., Takeuchi M., Zhang J., Horiuchi Y., Anpo M., Bahnemann D.W., 2014, Understanding TiO₂ photocatalysis: mechanisms and materials, *Chem. Rev.*, 114, 9919-9986.
- Stoller M., Vuppala S., Cheng K., Traore M., Marchetti A., Kanaev A., Chiavola A., 2019, Design of novel equipment capable to quickly produce efficient nanomaterials for use in environmental and sanitary emergencies, *Chem. Eng. Trans.* 73, 187-192.
- Su J., Zou X-X., Li G-D., Wei X., Yan C., Wang Y-N., Zhao J., Zhou L-J. and Chen J-S., 2011, Macroporous V₂O₅-BiVO₄ composites: Effect of heterojunction on the behavior of photogenerated charges, *J. Phys. Chem.*, 115, 8064-8071.
- Teramura K., Ohuchi T., Shishido T., Tanaka T., 2009, Study of the reaction mechanism of selective photooxidation of cyclohexane over V₂O₅/Al₂O₃, *J. Phys. Chem.*, 113, 17018-17024.
- Zaleska A., Doped-TiO₂: A review, 2008, *Recent Patents Eng.*, 2, 157-164.